Beyond Constriction Resistance: Multicomponent Microscale Conduction Model

B. Agrawal[1], M. Goldmann[2], M. Grott[1], J. Blum[3], J. Biele[4], C. Güttler[2], B. Gundlach[2], J. Kollenberg[1], and A. Greshake[5]

[1]German Aerospace Center, Berlin, Germany, [2]University of Münster, Germany, [3]Technische Universität Braunschweig, Germany, [4]Germany Aerospace Center, Cologne, Germany, [5]Museum für Naturkunde, Berlin, Germany

Before interpreting thermal infrared observations from missions like *Hayabusa2* and *OSIRIS-REx* [1, 2], we require accurate models of porous asteroids boulders. These materials originate as granular aggregates whose microstructures evolve through processes such as sintering, growing the inter-particle necks that govern bulk thermal conductivity and strength. Current DEM frameworks simplify contact conduction by assuming small contacts and classical constriction resistance alone. This reliance requires empirical fitting. Here, we implement a multicomponent microscale model in LIGGGHTS [3] resolving four distinct contact heat transport mechanisms, creating a predictive framework validated against laboratory sintering experiments [4].

Contact Heat Transport

Spherical particle of radius r_p in contact with another particle. They share a circle of contact of radius r_c. The material conductivity of the particles is assumed to be k_m. We consider four resistance mechanisms.

(a.) Constriction Resistance [5]:
As heat flows through a small space ($r_c \ll r_p$)

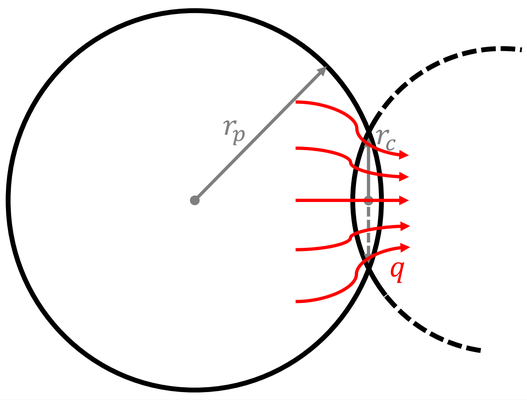

$$R_c = \frac{1}{4k_m r_c}$$

(b.) Constriction Alleviation Factor, Ψ [6]:
Reduction in resistance as the contact radius grows

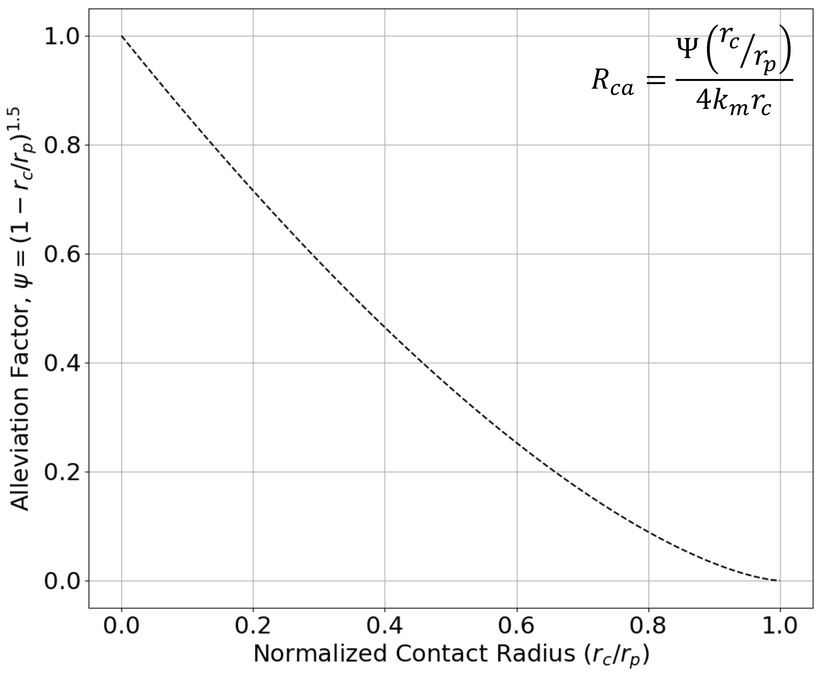

$$R_{ca} = \frac{\Psi\left(r_c/r_p\right)}{4k_m r_c}$$

(c.) Grain Boundary Resistance [7]:
As heat transfers across grain boundaries

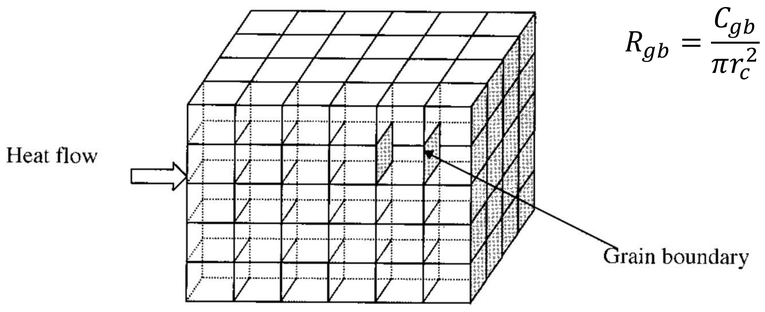

$$R_{gb} = \frac{C_{gb}}{\pi r_c^2}$$

(d.) Particle Bulk Resistance [8]:
Depends on the path length of heat inside the particle. Described by $F_1(r_c/r_p)$ and $F_2(\beta)$ that depend on contact radius ratio and contact angle respectively.

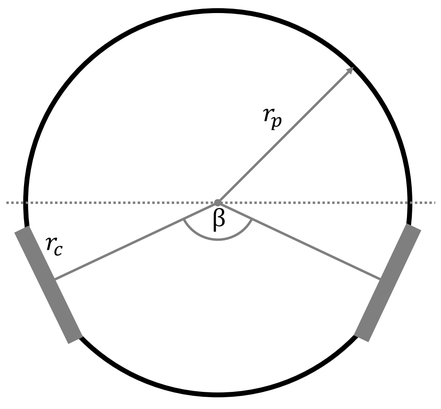

$$R_{pb} = \frac{F_1(r_c/r_p)}{k_m r_p} + \frac{F_2(\beta)}{k_m r_p}$$

Scale Dependence

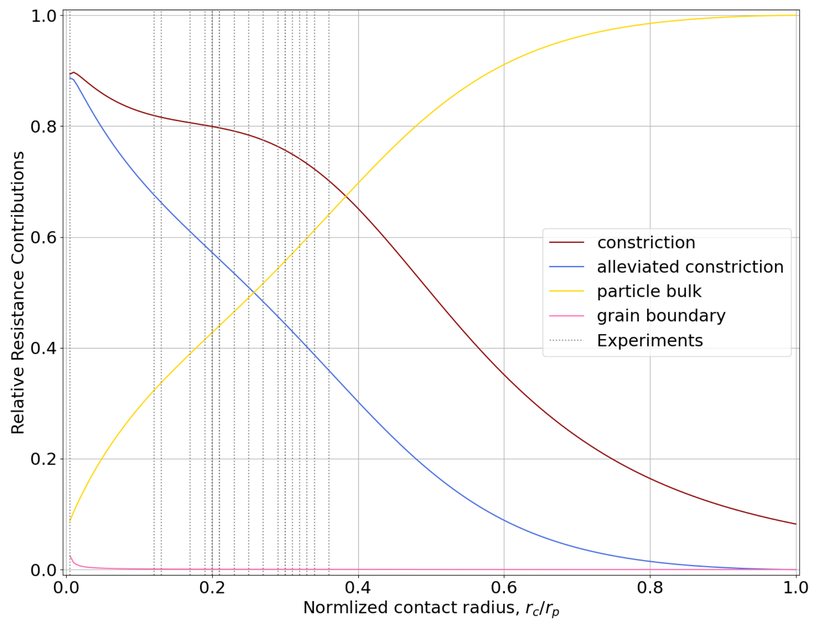

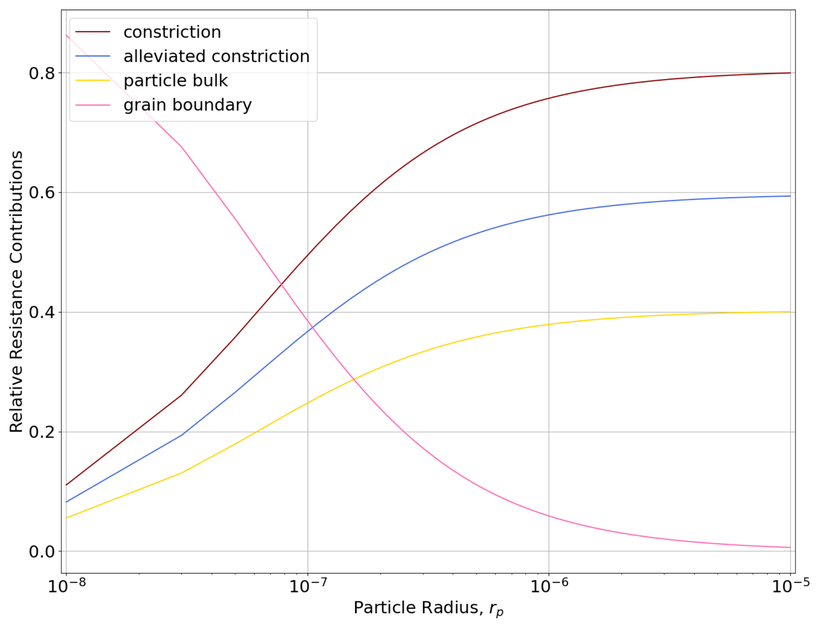

The figures show the relative contributions of different heat transport mechanisms to total contact resistance as a function of overlap (r_c/r_p) (left) and particle radius r_p (right), with the different colors representing the respective mechanisms. In left figure, $r_p = 100\mu m$ and we observe the effect of growing contact radius on resistance contributions. The grey dotted vertical lines mark the normalized contact radius values corresponding to those obtained in experiments with sintered glass beads [4]. The **particle bulk resistance** start small but **increases beyond constriction resistance as the particle overlap increases**. In figure on right, we fix $r_c/r_p = 0.18$ and observe the resistance contributions as the particle size increases. The **contributions approach a stable value and are effectively constant** for $r_p > 10\mu m$.

Simulations

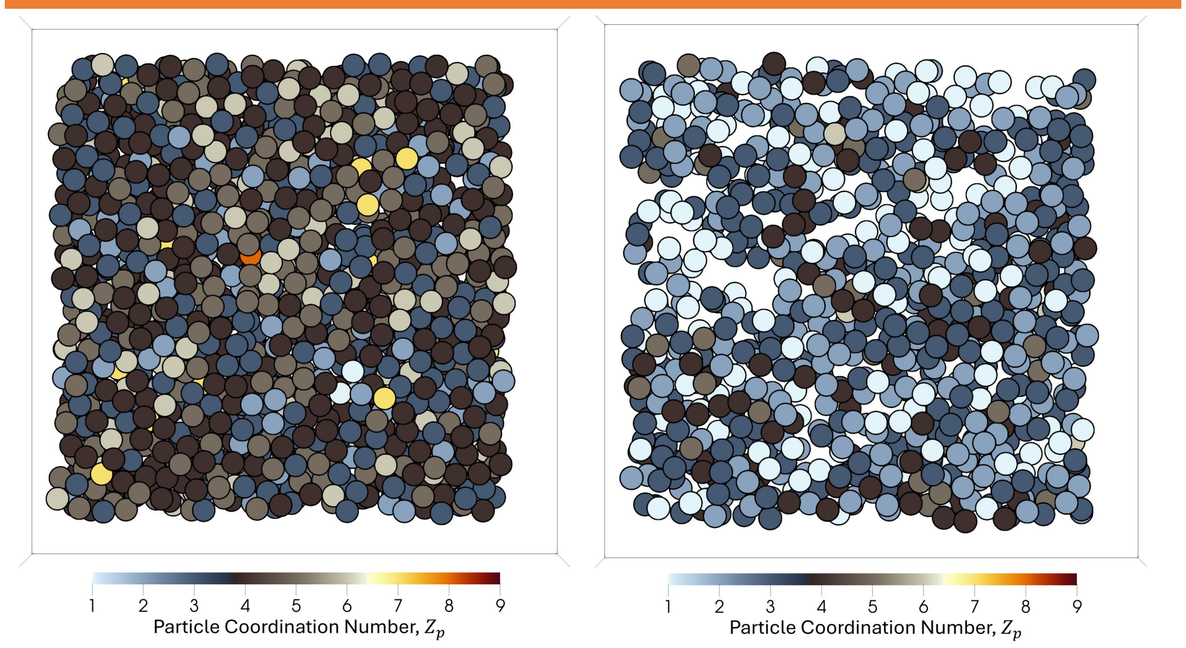

Experiments

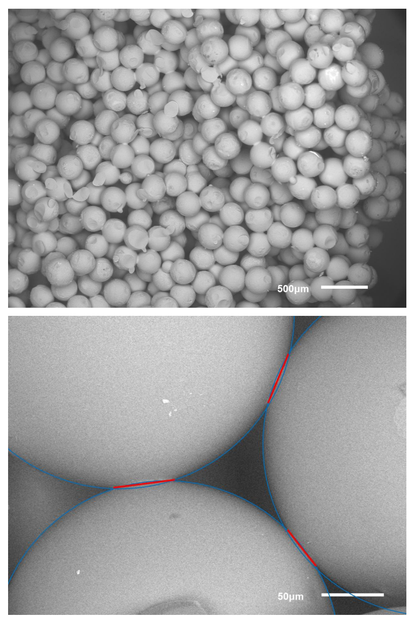

Presented in the set of figures on the left are the different porosity and coordination number aggregates used for **thermal analysis as detailed in Agrawal *et al.* (2026)**. An analogous experimental study is conducted by [4] with **soda lime glass beads** with similar porosities and varying degrees of sintering. Set of figures on the right show the SEM images of **sintered sample for thermal experiments.** The sintered neck between glass beads has been highlighted with a red line. A **comparison between our DEM simulations and thermal experiments** from [4] is established **at similar porosity and contact radius** to study the effect of contact resistance mechanisms on effective bulk conductivity.

Bulk Thermal Conductivity: Simulations and Experiments

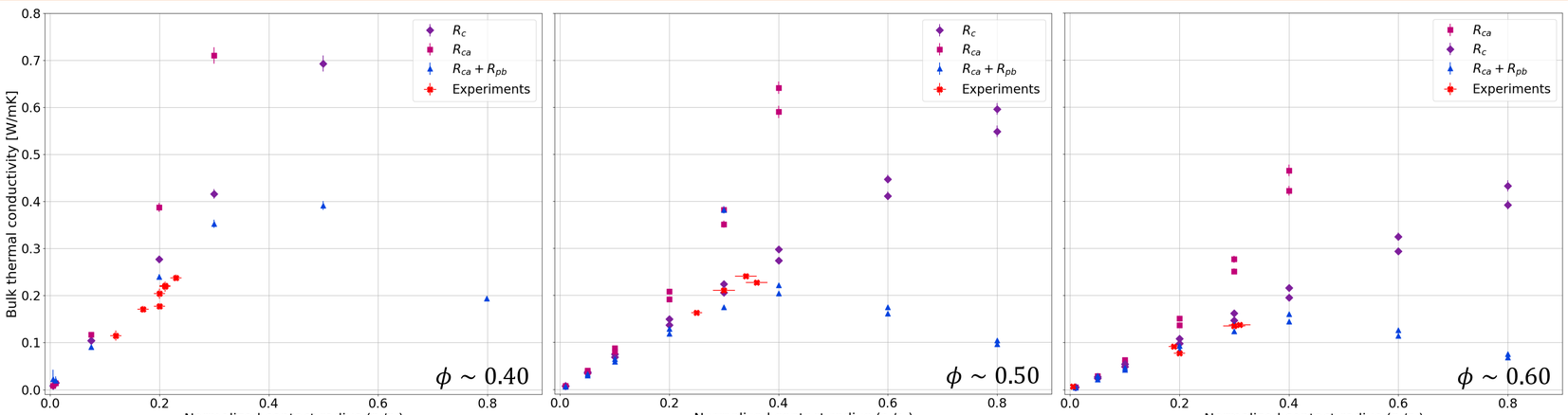

The figures showcase the bulk thermal conductivity from DEM simulations (colored points) and the experimental measurements [4] (red crosses). The different colored points represent the mechanisms included: constriction (purple diamond), constriction with alleviation (magenta square), alleviated constriction with particle bulk resistances (blue triangle). The three plots show the different porosity samples studied, going from low $(\phi \sim 0.40)$ to high porosity $(\phi \sim 0.60)$.

Key Results

- **Grain boundary resistance** has little to **no effect** on the bulk thermal conductivity in our study.
- **Constriction resistance** based thermal models are **only valid for very small overlaps** $(r_c/r_p \ll 1)$. Alleviation factor accounts for the decrease in resistance as overlap increases.
- **Alleviated constriction resistance** model **overshoots** the reduction in particle thermal resistance.
- **Particle bulk resistance** plays an **important role** in models with alleviated constriction resistance.

Conclusion, Caveat, Continuation…

- **Two models** – (i) constriction and (ii) alleviated constriction with particle bulk resistance, are **consistent with the experiments**.
- **More experimental measurements needed** but increasing overlaps without influencing sample porosity not possible. **Sintering causes densification of sample**.
- Sintering morphs the spherical beads out of shape. This **limits the applicability of current DEM models** for highly sintered glass beads.

References

[1] Okada et al., Space Sci Rev 2017, 208, 255-286. [2] Lauretta et al., Space Sci Rev 2017, 212, 925-984. [3] Kloss et al., Progress in Computational Fluid Dynamics 2012, 12, 140-152. [4] Goldmann et al. (2026), EPSC2026-570. [5] Madhusudana (2016), Thermal Contact Conductance, Springer. [6] Cooper et al. (1969), International Journal of Heat and Mass Transfer, 12, 279–300. [7] Smith et al. (2003), Journal of the American Ceramic Society, 86, 105–111. [8] Siu and Lee (2000), International Journal of Heat and Mass Transfer, 43, 3917–3924. [9] Agrawal et al. (2026), Planetary Science Journal, 7, 142.

Acknowledgments. This project is funded by DFG grant GR 3751/2-1 with the title '*Thermal and Mechanical Properties of Carbonaceous Chondrites*'.